Engineering Structures 66 (2014) 81–88

Contents lists available at ScienceDirect

Engineering Structures

journal homepage: www.elsevier.com/locate/engstruct

Experimental and numerical investigations of buckle interaction in subsea pipelines

Hassan Karampour, Faris Albermani *

School of Civil Engineering, The University of Queensland, Australia

ARTICLE INFO

Article history:
Received 18 July 2013
Revised 9 January 2014
Accepted 22 January 2014
Available online 5 March 2014

Keywords:
Buckle-interaction
Buckle propagation
Upheaval buckling
Subsea pipelines

ABSTRACT

Experimental and finite element results for buckle interaction in subsea pipelines are presented in this paper. Experimental results for buckle propagation and pure bending of pipes are presented first followed by buckle interaction results. A finite element model, verified against the experimental results, is used to develop buckle interaction envelopes. The analysis is conducted using both transient and steady state conditions. The results highlight the vulnerability of subsea pipelines to buckle interaction particularly in deep waters.

1. Introduction

The diminishing onshore hydrocarbon reserves have resulted in an unprecedented increase in deep subsea operations. Hydrocarbon production in deep water requires long pipelines and the design of such pipelines poses many engineering challenges and potential risk [1].

A long pipeline may experience global buckling through lateral or upheaval buckling modes [2]. Although these two buckling modes are not essentially failure modes, they can precipitate failure through excessive bending that may lead to fracture, fatigue or propagation buckling.

In deep water, pipelines are susceptible to catastrophic propagation buckling [3]. Buckle propagation is a snap-through phenomenon that can be triggered by a local buckle [4], ovalization, dent or corrosion in the pipe wall. The resulting buckle quickly transforms the pipe cross-section into a dumb-bell shape that travels along the pipeline as long as the external pressure is high enough to sustain propagation. Fig. 1 shows a typical buckle propagation response depicted in terms of the applied external hydrostatic pressure against the pipe's volume change ($\Delta V/V$) and is characterised by the pressure at which the snap-through takes place (the initiation pressure P_I) and the pressure that maintains propagation (the propagation pressure P_p) which is a small fraction of P_I. The elastic collapse pressure, P_{el}, represents an upper-bound on P_I while Palmer and Martin [5] pressure, P_{PM}, gives a lower-bound on P_p. These two pressures, P_{el} and P_{PM}, are given by

$$P_{el} = \frac{2E}{(1-\nu^2)}\left(\frac{t}{D}\right)^3 \tag{1}$$

$$P_{PM} = \pi\sigma_y\left(\frac{t}{D}\right)^2 \tag{2}$$

Unlike propagation pressure P_p, the initiation pressure P_I is very sensitive to initial imperfection such as local dents or ovalizations [3,6,7]. In this work ovality Ω is defined as

$$\Omega = (D_{\max} - D_{\min})/D \tag{3}$$

In deep waters, buckle interaction between lateral or upheaval buckling and propagation buckling need to be accounted for in the design of pipelines. So far, buckle interaction in deep subsea pipelines has received limited attention [8,9].

Two aluminium (alloy 5052-0) pipes with D/t = 28.57 and 42.86 are used in this study as shown in Table 1. Two longitudinal tensile coupons and two compressive stub tests (Fig. 2) were conducted for each D/t to determine the material yield stress and elasticity modulus listed in Table 1.

Experimental and numerical investigation of buckle interaction in pipelines is presented in this paper. For this purpose, experimental results for propagation buckling and pure bending of pipes are presented first followed by the results for buckle interaction. The paper concludes by presentation of interaction envelopes and a comparison with relevant design standards.

* Corresponding author. Tel.: +61 7 33654126.
E-mail address: f.albermani@uq.edu.au (F. Albermani).

http://dx.doi.org/10.1016/j.engstruct.2014.01.038
0141-0296/

Nomenclature

D	nominal outside diameter of pipe	k	curvature
D_0	pipe mean diameter, $D_0 = D - t$	k_c	critical curvature
D_{max}	measured maximum outside diameter of pipe	V	pipe's volume
D_{min}	measured minimum outside diameter of pipe	ΔV	change in pipe's volume due to external pressure
t	pipe wall thickness	Ω	ovalization ratio
E	modulus of elasticity	a_o	wrinkle imperfection base amplitude
E_t	tangent modulus of elasticity	a_i	wrinkle amplitude bias
v	Poisson's ratio	λ	wrinkle imperfection half-wave length
σ_y	yield stress	N	number of half-waves in wrinkle imperfection
M_p	plastic moment	$\bar{\omega}$	localised wrinkle imperfection
P_I	buckle initiation pressure	p_e	external pressure (used in DNV)
P_p	buckle propagation pressure	γ_m, γ_{sc}	partial resistance factors in DNV
P_{el}	elastic collapse pressure	f_0	ovalization ratio according to the DNV
P_{PM}	Palmer and Martin propagation pressure	f_y	yield stress in DNV
p	external pressure	M_{SD}	design moment
p_I	experimentally obtained buckle initiation pressure in buckle interaction tests	S_{SD}	design effective axial force
		α_{fab}	fabrication factor in DNV
P_I^{FE}	FE buckle initiation pressure	α_c	flow stress parameter in DNV

2. Buckle propagation

Buckle propagation tests were conducted using 4 m long hyperbaric chamber shown in Fig. 3a. The protocol for hyperbaric chamber testing is described by Khalilpasha and Albermani [6]. Pipe specimens 1.8 m long were used and two tests were conducted for each D/t. A typical hyperbaric chamber test result is shown in Fig. 1 in terms of the applied external hydrostatic pressure against the volumetric change, $\Delta V/V$, of the tested pipe specimen.

Prior to the conduct of the hyperbaric chamber test, the initial ovalization of each test specimen was measured along the pipe's length using a laser position sensor mounted on a rigid frame as shown in Fig. 3b. The ovalization is measured at 37 sections along the pipe (at 50 mm intervals). At each section, five measurements around the pipe's circumference were recorded to determine D_{min} and D_{max} and hence Ω (Eq. (3)) is calculated for that section. Table 2 gives the largest ovalization measured for each specimen prior to testing. The P_I and P_p results obtained from the hyperbaric chamber tests are also shown in Table 2. Fig. 4a shows the pipe specimens after the hyperbaric chamber test. The extent of buckle propagation can be clearly seen in this figure.

Nonlinear finite element simulation of buckle propagation is conducted using ANSYS [10]. The FE model is composed of thin shell, frictionless contact and target elements (ANSYS elements 181, 174 and 170 respectively). The target/contact elements are used to define the contact between the inner surfaces of the pipe wall as it deforms into a dog-bone shape (Fig. 4b). A von-Mises elastoplastic material definition with isotropic hardening and seven through-thickness integration points are used. The full-length (1.8 m) of the pipe specimen is modelled. One half (π) of the pipe in the circumferential direction is discretised using 40 shell elements. Initial ovalization at a section along the pipe model is introduced by conducting a linear analysis under a patch external pressures over an area one D long and $\pi/10$ wide in the circumferential direction. The patch load is adjusted to obtain the measured ovalization from the experiment (Table 2). The updated geometry is then used in the following nonlinear analysis to simulate buckle propagation.

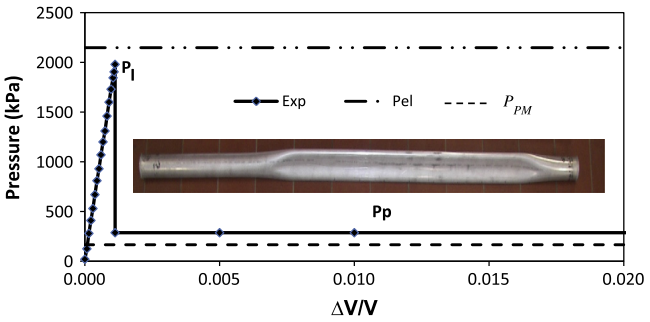

Fig. 1. Hyperbaric chamber test results of buckle propagation response (D/t = 42.86, Ω = 0.15%, 1.8 m long pipe).

Table 1
Properties of the pipe specimens used in the study.

D/t	D (mm)	t (mm)	E (GPa)	$\frac{E_t}{E}$	σ_y (MPa)	$\frac{\sigma_y}{E}$	M_P (kN mm)
42.86	38.10	0.90	69.0	0.0217	90	0.013	110.79
28.57	25.40	0.90	69.0	0.0217	90	0.013	48.07

The initiation and propagation, P_I^{FE} and P_p^{FE}, results from the FE analysis for the measured Ω and for an intact pipe (Ω = 0) are listed in Table 2. The results in Table 2 show good agreement (±5%) between the FE predictions and experimental results for both P_I and P_p. The results also highlight the sensitivity of P_I (but not P_p) to initial imperfection. Using an initial ovalization Ω of 0.1% and 1% for D/t = 42.86 and 28.57 respectively, the normalised FE propagation response is shown in Fig. 5.

Fig. 6 shows the results from a FE parametric study on imperfection sensitivity of buckle initiation. The reduction in P_I of imperfect pipe ($\Omega > 0$) relative to intact pipe (Ω = 0, Table 2) is shown together with the obtained experimental results. It can be seen that the initial ovalization of Ω = 1% measured in the experiment has resulted in a drastic reduction in P_I of 18% and 28% for the thin and tick pipes respectively. The results shown in Fig. 6 indicate that thicker pipes, which are more suitable for deep subsea applications, are more sensitive to imperfection.

3. Pure bending

Under upheaval and lateral buckling, the pipeline is subjected to excessive bending [2]. For this reason an experimental investiga-